Magnetic Resonance Imaging 63 (2019) 137–146

Contents lists available at ScienceDirect

Magnetic Resonance Imaging

journal homepage: www.elsevier.com/locate/mri

Technical Note

Free-breathing non-contrast-enhanced flow-independent MR angiography using magnetization-prepared 3D non-balanced dual-echo Dixon method: A feasibility study at 3 Tesla

Masami Yoneyama[a], Shuo Zhang[b,c,*], Houchun Harry Hu[d], Le Roy Chong[e], Dianna Bardo[f], Jeffrey H. Miller[f], Nobuyuki Toyonari[g], Kazuhiro Katahira[g], Yasutomo Katsumata[h], Amber Pokorney[f], Chian Keat Ng[c], Marc Kouwenhoven[h], Marc Van Cauteren[h]

[a] Philips Japan, Philips Building, 13-37 Kohnan 2-chome, Minato-ku, Tokyo 108-8507, Japan
[b] Philips Healthcare, Roentgenstrasse 22-24, 22335 Hamburg, Germany
[c] Philips Singapore, 622 Lorong 1, Toa Payoh 319763, Singapore
[d] Nationwide Children's Hospital, 700 Children's Dr, Columbus, OH 43205, USA
[e] Changi General Hospital, 2 Simei Street 3, 529889, Singapore
[f] Phoenix Children's Hospital, Arizona, 1919 E Thomas Rd, Phoenix, AZ 85016, USA
[g] Kumamoto Chuo Hospital, 1 Chome-5-1, Tainoshima, Minami Ward, 862-0962 Kumamoto, Japan
[h] Philips, Veenpluis 6, 5684 PC Best, the Netherlands

ARTICLE INFO

Keywords:
Non-contrast-enhanced MR angiography
Dual-echo generalized Dixon
Magnetization preparation
Flow independent
Free breathing
Whole-body

ABSTRACT

In this work we aimed to investigate the feasibility of using a new pulse sequence called Relaxation-Enhanced Angiography without Contrast and Triggering (REACT) for free-breathing non-contrast-enhanced MR angiography (NCE-MRA) for multiple anatomies on 3T. Two magnetization-preparation pulses were incorporated with a three-dimensional dual-echo Dixon sequence. A T2-prep pulse, followed by a non-selective inversion pulse with a short inversion time, together suppressed tissue with short T1 and T2, while enhancing the signal of native blood with long T1 and T2. A two-point non-balanced gradient-echo Dixon method, based on dual-echo acquisition with semi-flexible echo times for water-fat separation, was used for improved fat suppression over a large field of view. General image quality, vasculature visibility, and clinical indications of the proposed method were investigated in healthy subjects and patients in both torso and extremities based on visual inspection. Preliminary results from REACT obtained in free-breathing with no cardiac triggering showed uniform suppression of background tissue over the field of view and robust blood-to-tissue contrast over multiple anatomies. Future clinical studies are warranted for further investigation of its diagnostic performance and limitations.

1. Introduction

Magnetic resonance angiography (MRA) has a wide range of clinical applications for assessment of vascular morphology and pathology, and has the advantage of being minimally invasive with no ionizing radiation exposure. Contrast-enhanced (CE) MRA is an established approach that uses gadolinium-based contrast agent to reduce the T1 of blood and to generate hyperintense blood signal in the angiogram [1,2]. Although it has shown excellent performance in diverse applications [3], a remaining technical challenge is the limited acquisition window to capture the first-pass of the contrast agent bolus, affecting the achievable spatial resolution [4,5]. Beyond that, safety concerns regarding gadolinium contrast media [6,7] have led to a renewed interest in non-contrast-enhanced (NCE) MRA techniques that may be repeated multiple times within a single examination or over a short time period without the restrictions of dose limits [8].

In NCE-MRA, contrast between blood and other tissues is generated by exploiting either differences in relaxation time [9–11] or flow characteristics [12–15]. The latter relies on the property that blood is flowing – moving over time – distinguishing it from the surrounding tissues. However, such techniques typically suffer from image quality issues related to variable flow rates and directions [12,13], sensitivity to timing between data acquisition and cardiac phases [14,15], or bulk motion between two consecutive measurements for subtraction [15].

On the other hand, in non-contrast-enhanced flow-independent MRA (NCE-FIA), intrinsic tissue parameters such as relaxation times

* Corresponding author at: Clinical Science MR, Health Systems, Philips Healthcare, Röntgenstraße 24, 22335 Hamburg, Germany.
E-mail address: zhangshuo517@gmail.com (S. Zhang).

https://doi.org/10.1016/j.mri.2019.08.017
Received 26 March 2019; Received in revised form 18 July 2019; Accepted 15 August 2019

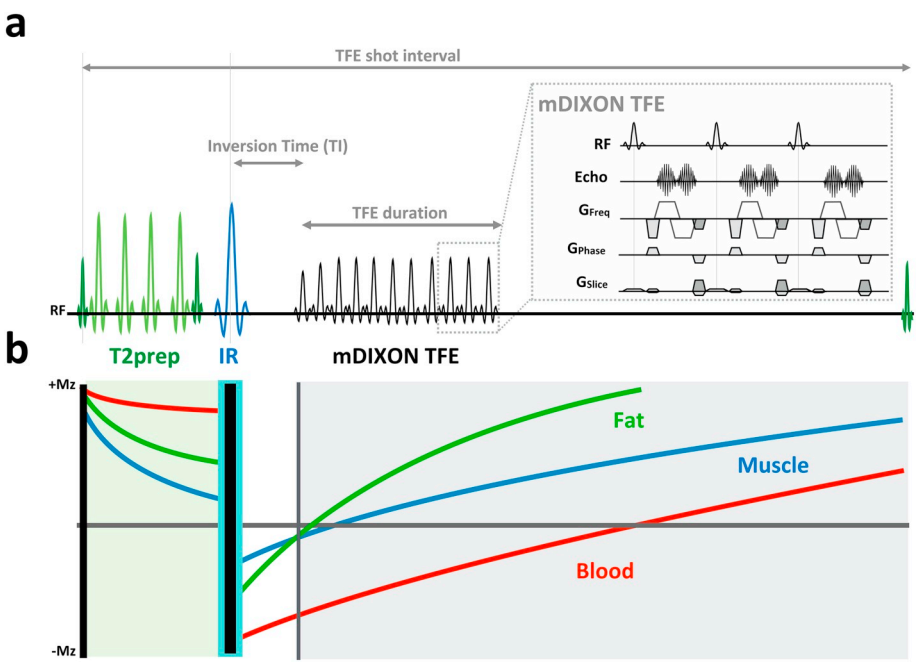

Fig. 1. Principle of 3D REACT vascular imaging. The pulse sequence diagram (**a**) illustrates key modules of the technique, namely, magnetization preparation pulses of non-selective T2-prep and inversion recovery (IR), and data acquisition using 3D dual-echo Dixon with non-balanced turbo-field echo (TFE) in centric k-space profile ordering. An estimated signal evolution of different tissue types (**b**) demonstrates that data acquisition occurs after a short inversion time (TI) when signal from background tissues such as muscle crosses the null point and are thus suppressed, while blood is further enhanced with residual fat signal suppressed by the dual-echo generalized Dixon method. For details see text.
mDixon TFE = modified dual-echo generalized Dixon with segmented non-balanced turbo field echo.

Table 1
Imaging parameters of the pulse sequences used in the present study.

	REACT	3D TOF-MRA	2D TOF-MRA	bSSFP-MRA	TRANCE	CE-MRA
Anatomies	Subclavian, thorax, abdomen and pelvis, extremities	Subclavian	Pelvis and femur	Subclavian, thorax, abdomen	Femur	Pelvis, extremities
FoV [mm^2]	280 × 280	280 × 280	400 × 280	280 × 280	280 × 280	430 × 300
Slice orientation	Coronal	Axial	Axial	Coronal	Coronal	Coronal
Number of slices	80	350	160	80	80	80
Voxel size (ACQ) [mm^3]	1.2 × 1.2 × 2.4	1.2 × 1.2 × 2.0	1.5 × 2.3 × 3.5	1.2 × 1.2 × 2.4	1.2 × 1.2 × 2.4	1.2 × 1.2 × 2.4
Voxel size (REC) [mm^3]	1.0 × 1.0 × 1.2	1.0 × 1.0 × 1.0	1.0 × 1.0 × 3.5	1.0 × 1.0 × 1.2	1.0 × 1.0 × 1.2	1.1 × 1.1 × 1.2
Magnetization preparation	T2-prep, IR	–	–	–	IR	–
T2prep time [ms]	50	–	–	–		–
Inversion delay time [ms]	100	–	–	–	180	–
Fat suppression	mDixon	–	–	SPIR	STIR	Subtraction
Signal readout	3D TFE	3D FFE	2D FFE	3D bTFE	3D TSE	3D T1 FFE
TR/TE [ms]	3.9/1.38/2.5	18/3.5	18/3.5	4.0/2.0	1 heartbeat/100	4.7/2.3
Flip angle [°]	12	18	50	60	90	25
Turbo factor	100	–	–	77	21	–
# TFE shot	80	–	–	–	–	–
TFE shot interval [ms]	3000	–	–	2000	–	–
Motion compensation	None	None	Cardiac triggering	None	Cardiac triggering	None
Partial-Fourier factor	0.625 to 0.85	1.0	0.75	0.625 to 0.8	1.0	0.625
SENSE factor	1.2 to 2.5	3.0	4.0	1.2	4.0	2.0
NSA	1	1	1	1	1	1
Scan time [min]	2:30 to 4	8:11	5:22	3:37	5:32	0:53

REACT = relaxation-enhanced angiography without contrast and triggering, TOF = time of flight, TRANCE = ECG-triggered non-contrast-enhanced MR angiography, TFE = turbo-field echo, FFE = fast field echo, SENSE = sensitivity encoding, ACQ = acquired, REC = reconstructed, mDixon = modified dual-echo generalized Dixon; NSA = Number of signal average; CE-MRA = contrast-enhanced MRA.

and chemical shift are utilized to suppress background signals and generate relatively stable vessel contrast [16,17]. To date the balanced steady-state free precession (bSSFP) sequences have been of particular interest due to their high signal amplitude and blood-to-tissue contrast. However, the main drawback of the bSSFP-based technique is its sensitivity to off-resonance effects and field inhomogeneities. Thus image quality can be degraded by banding artifacts, signal loss, or insufficient fat suppression, particularly for a large field-of-view (FOV) or at high field strength [10,11,18–21].

In this work, we developed a new NCE-FIA technique with Relaxation-Enhanced Angiography without Contrast and Triggering (REACT) to address the aforementioned limitations. This method is based on 3D magnetization-prepared dual-echo generalized Dixon with a non-balanced gradient-echo readout. It allows for high blood-tissue-contrast with robust and efficient background tissue suppression covering large and complex anatomies, without the need for physiological triggering or subtraction. In this proof-of-concept study we demonstrated the technical feasibility of REACT in comparison to conventional flow-dependent techniques such as time-of-flight (TOF) and ECG-triggered non-contrast-enhanced MR angiography (TRANCE) as well as flow-independent ones such as 3D balanced steady-state free-precession (bSSFP) with fat saturation in various anatomies at 3 Tesla.

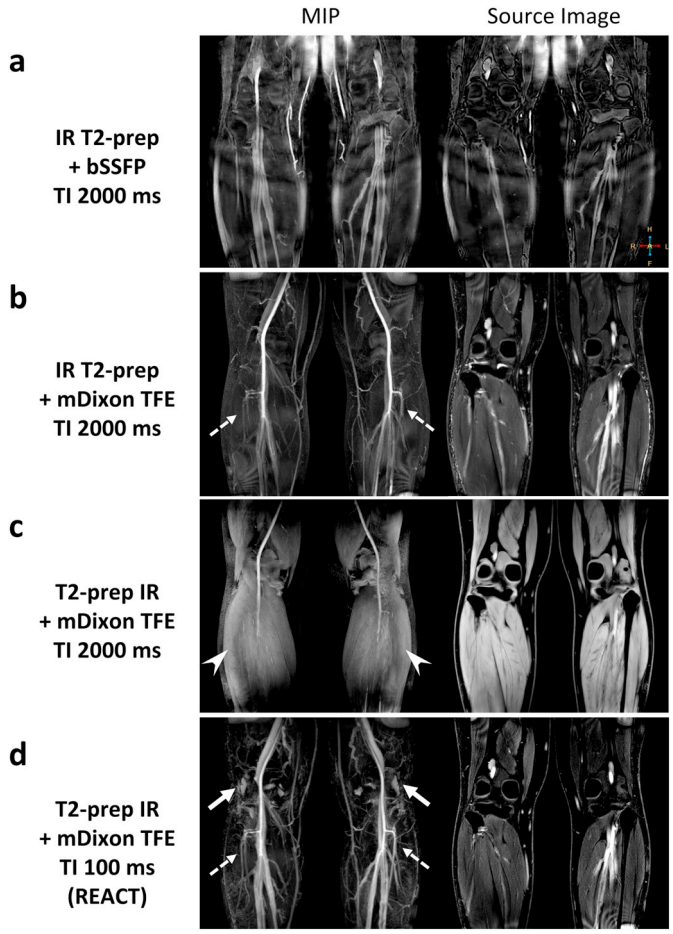

Fig. 2. Comparison of basic variants in NCE-flow-independent MRA using magnetization-preparation. Signal readout with bSSFP (a) showed heterogeneous background tissue suppression due to present field inhomogeneities in comparison to the non-balanced variants based on dual-echo generalized Dixon (b–d). While a long inversion time (TI) following the inversion-recovery (IR) pulse (a–c) demonstrated superior suppression of long-T1 tissue species such as synovial fluids in the knee (arrows) comparing to the short-TI variant (d), its variant with a directly inverted temporal order of the two magnetization-preparation pulses (c) failed background tissue suppression due to signal contamination from short-T2 tissue species such as skeletal muscles (arrow heads). Lastly, a preceding T2-prep pulse in combination of a short TI (d) presented the best quality in terms of uniformity and blood-tissue-contrast (dotted arrows), which comprised the proposed REACT method in this work.
mDixon TFE = modified dual-echo generalized Dixon with segmented non-balanced turbo field echo.

2. Materials and methods

2.1. 3D dual-echo Dixon with T2- and IR-preparation

The pulse sequence for the proposed REACT method consisted of a 3D dual-echo Dixon acquisition and magnetization preparation with a T2-prep pulse and a non-selective inversion recovery (IR) pre-pulse. The Dixon acquisition was based on an improved generalized 2-point solution with semi-flexible echo times (TE) for water-fat separation that was introduced previously [22]. It removed the need for specified TE to meet the exact in- and opposed phase condition, which is dependent on the field strength and limited by voxel size [22,23]. In addition, a priori knowledge of magnet and anatomy were incorporated to improve B0 inhomogeneity correction and overall water-fat separation performance [24]. This was further combined with a seven-peak fat model in reconstruction to achieve improved accuracy [25,26]. All these features helped to eliminate the usual limitations of the conventional Dixon acquisition in echo times, spatial resolution, anatomical coverage, and scan time, while maintaining robust water-fat separation [22,23,27].

Magnetization preparation pulses were implemented to suppress signal from static tissues, such as muscles, nerves and organs, and to enhance blood-to-tissue contrast based on their difference in relaxation times. A T2-prep pulse consisting of four adiabatic refocusing pulses was applied to reduce signal from tissues with short T2 [28]. Immediately after that a non-selective, adiabatic inversion recovery pulse was applied with a short inversion time (TI) to suppress tissues with short-to-intermediate T1 and T2 such as muscle [29]. Data acquisition was done by the aforementioned Dixon readout that allowed for effective fat suppression in the water images. This combined effect of background tissue suppression including fat resulted in an enhanced visualization of the vasculature. A simplified pulse sequence diagram of the proposed REACT method is presented in Fig. 1.

2.2. Technical implementation and feasibility

3D data were acquired by a dual-echo non-balanced gradient-echo Dixon sequence with a bipolar gradient readout, and was segmented over a number of turbo field-echo (TFE) shots. Each shot was preceded by a T2-prep followed by an IR pulse. The duration of each TFE shot (i.e. turbo factor) was optimized for image quality and total acquisition time. This resulted in a typical turbo factor of 100 and a shot duration of approximately 400 ms. A quadratic ramp-up flip angle sweep was applied to reduce the transient-state signal oscillations [30]. In addition, centric k-space profile ordering was used in combination of half-Fourier and parallel imaging acquisition for data readout to achieve both shortened scan time and efficient background suppression, as the center of k-space was sampled when the signal from background tissues crossed the null point after a short inversion time (TI). Between each shot the magnetization is allowed to return to equilibrium with a typical interval time of 3000 ms, after which the magnetization preparation is repeated and the next shot is acquired (Fig. 1).

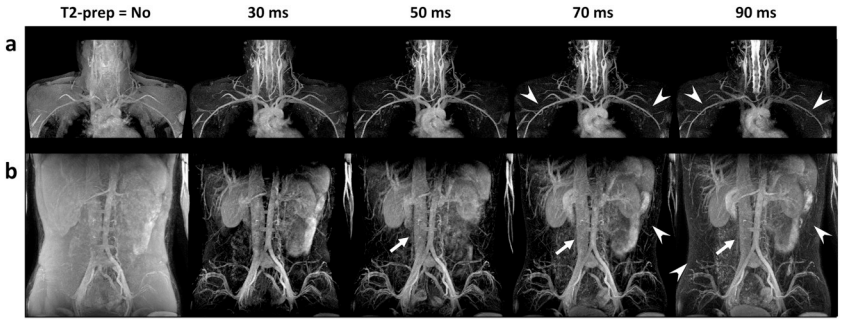

Fig. 3. Effect of T2-preparation pulse duration in REACT imaging. Images were acquired with a 3D IR-prepared Dixon TFE with an inversion time (TI) of 100 ms in subclavian (**a**) and abdominal (**b**) areas. While a longer T2-prep time led to a higher arteriovenous contrast, as seen typically between the abdominal aorta and inferior vena cava (arrows), it also resulted in increased signal intensity in background tissues and organs (arrow heads).

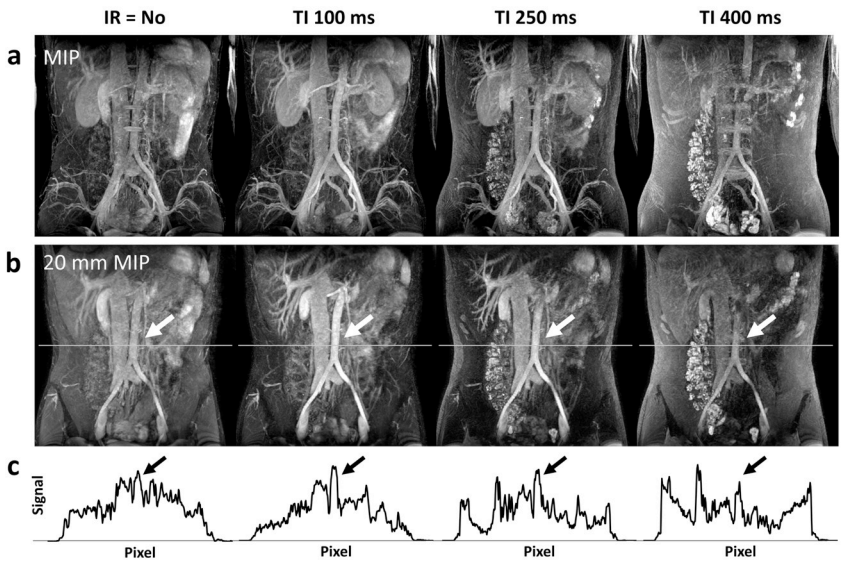

Fig. 4. Effect of the inversion time (TI) in REACT imaging. Images were acquired with a 3D T2-prepared Dixon TFE with a T2-prep time of 50 ms in abdomen (**a**). In general, higher background signal and lower blood-tissue-contrast was observed with an increased TI, which was better visualized from the corresponding 20 mm MIP images (**b**) and signal profiles (**c**), respectively. Abdominal aorta was indicated by the arrows in (**b**) and (**c**).

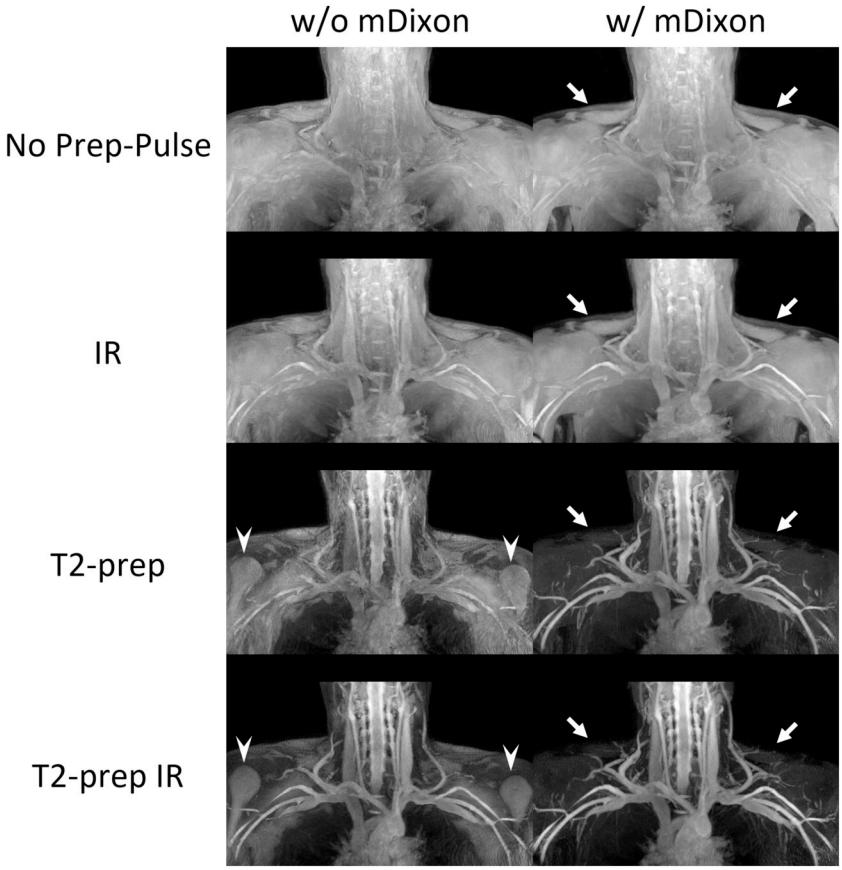

Fig. 5. Joint effect of the individual technical modules on final image appearance in REACT vascular imaging. All images shown are maximum intensity projections from the first echo acquisition (left) and water-only images (right) of the dual-echo generalized Dixon in a healthy subject in the subclavian area with a FOV of 460 × 460 mm. Dixon with non-balanced TFE acquisition provides homogeneous fat suppression over the entire FOV, particularly in the neck area, and subcutaneous (arrows) or bony (arrow heads) structures. A magnetization inversion recovery (IR) pre-pulse with a short inversion delay in combination with the Dixon method provides contrast between vessels and background tissues such as muscle based on differences in their T1 (second row). A magnetization T2-prep pulse in combination of the Dixon method renders high contrast between vessels and background tissues based on differences in their T2 (third row). Finally, the joint effect of both T2-prep and IR pulses with the Dixon method achieves the best overall background signal suppression, while enhancing the apparent blood signal in the vessels (last row). Consequently, the proposed REACT method was established for in vivo flow-independent relaxation-based angiographic imaging.
mDixon TFE = modified dual-echo generalized Dixon with segmented non-balanced turbo field echo.

2.3. Human imaging

Volunteer scans were performed on a 3T whole-body clinical system (Ingenia, Philips, Best, the Netherlands) using a 32-channel anterior and posterior phased-array coil. Ten healthy subjects (age 33 ± 7 years) without known diseases were scanned in multiple body parts. REACT was compared to several other NCE-MRA techniques. For the subclavian area flow-dependent NCE-MRA based on 3D time-of-flight (TOF) and flow-independent MRA based on 3D balanced steady-state free-precession (bSSFP) with fat saturation were additionally performed. Both techniques are commonly used in clinical practice in the upper body segment, with the former primarily in head and neck, while the latter is also used for abdomen. For pelvis and lower extremities flow-dependent NCE-MRA based on conventional 2D TOF and ECG-triggered non-contrast-enhanced MR angiography (TRANCE) were additionally performed [15,31]. These techniques are typically used in long vessels with ECG triggering to avoid motion-induced ghost artifacts or misalignment due to arterial signal variations. For thorax and abdomen the aforementioned bSSFP technique was also performed for comparison. All images were visually assessed for overall image quality. The typical imaging parameters of the pulse sequences used were summarized in Table 1.

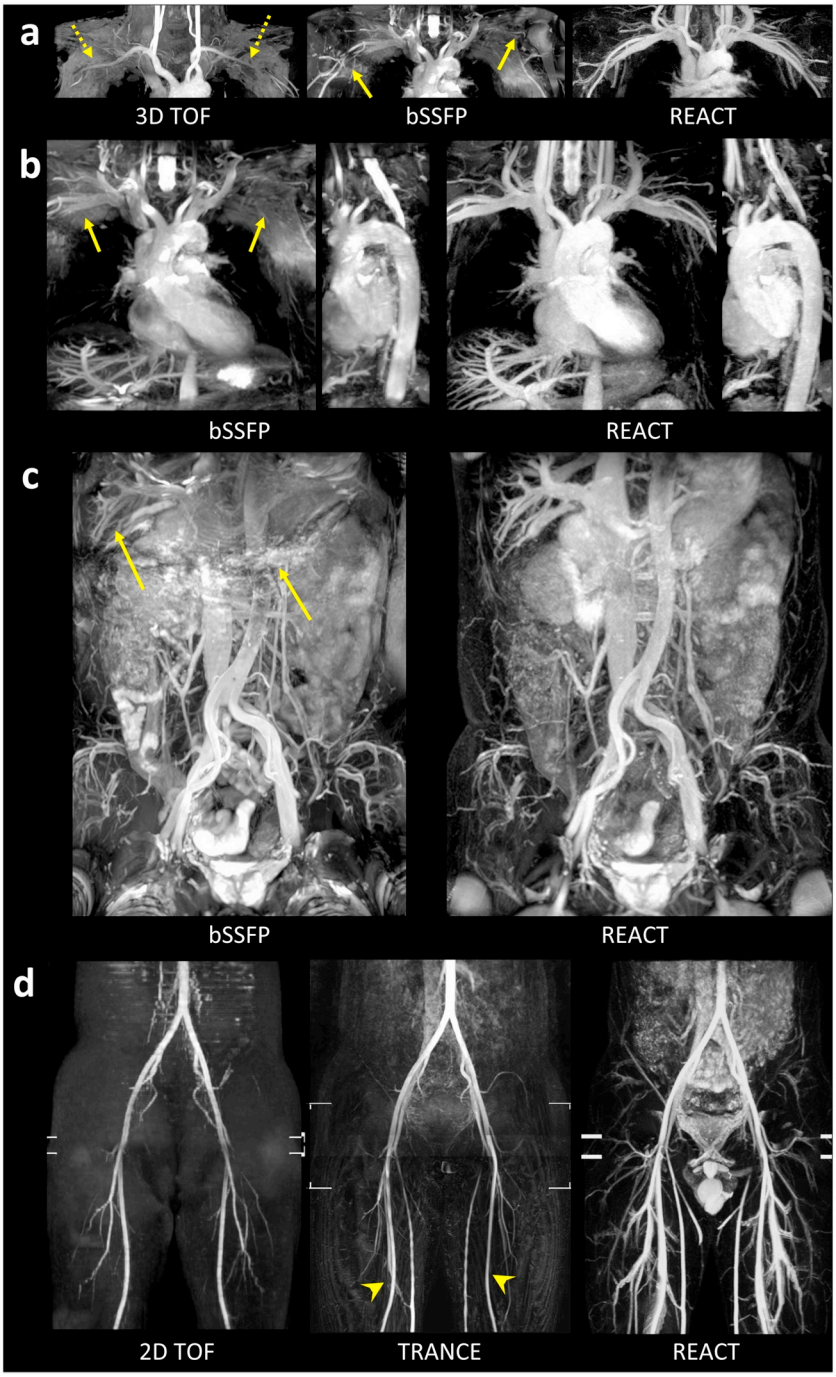

Fig. 6. REACT in healthy volunteers with comparison to conventional non-contrast-enhanced sequences TOF- and bSSFP-based MRA as well as TRANCE. Representative examples were selected from subclavian vessels (**a**), aorta (**b**), abdomen (**c**), and pelvic-femoral area (**d**). REACT showed the best image quality in general, and particularly, in terms of vessel conspicuity, despite relatively lower arterial selection. For details see text.

Moreover, patient scans were conducted by REACT with the same imaging parameters as used in the volunteers. Twelve patients with age ranging from 6 to 72 years old were studied with various vascular malformations or pathologies. The scan times were about 3 to 4 min in free breathing and without respiratory triggering. Images were visually assessed and compared between REACT and conventional CE-MRA. The latter was part of the standard patient scan protocol (imaging parameters in Table 1). In addition, tissue areas without lesion and with uniform signal were selected for quantitative measurement of contrast-to-noise ratio (CNR). This was defined by $CNR = (Mean_{blood} - Mean_{background})/(SD_{blood}^2 + SD_{background}^2)^{1/2}$, where Mean and SD refer to mean values and standard deviations of the signal intensity measured inside the lumen area (blood) and background avoiding artifacts, respectively [50]. Comparison of the results was performed by paired *t*-test analysis. A *p*-value of <0.05 was considered statistically significant. Both volunteer and patient scans were approved by the local ethics committee and all subjects gave written informed consent.

3. Results

3.1. Technical implementation and sequence optimization

For the feasibility test, a comparison of basic variants in NCE-FIA using magnetization-preparation was performed. As shown in Fig. 2,

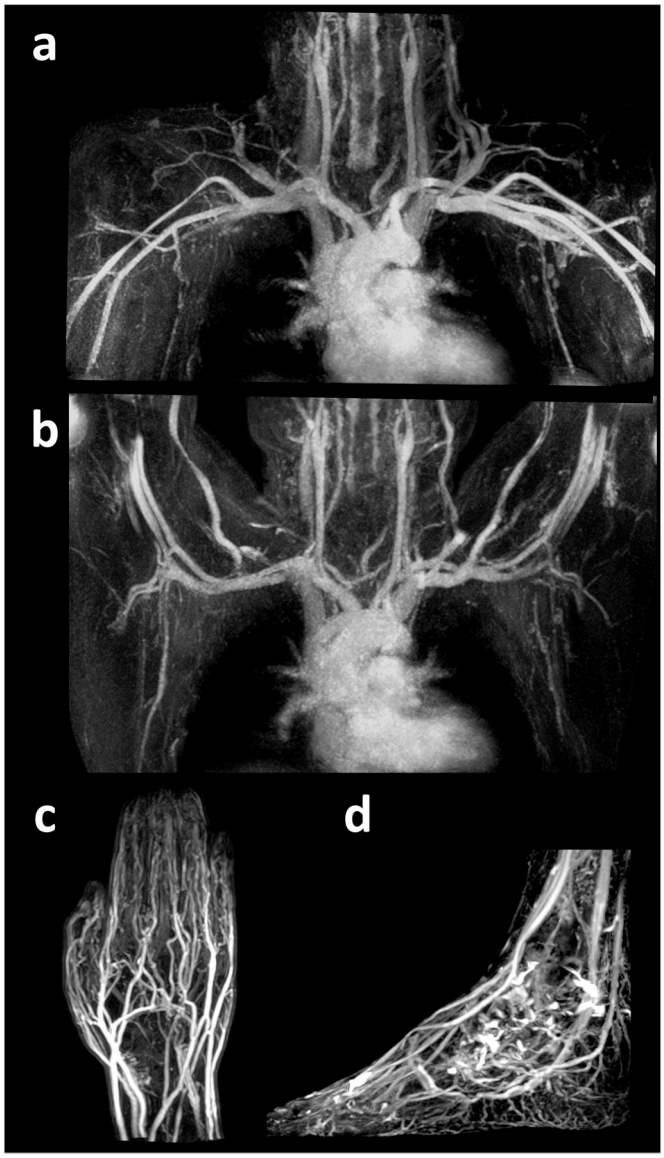

Fig. 7. REACT of the subclavian area in a neutral arm position without abduction (**a**) and an arm abducted position (**b**), of hand (**c**) and foot (**d**) in healthy volunteers.

signal readout with bSSFP (Fig. 2a) presented inhomogeneous background tissue suppression caused by present field inhomogeneities in comparison to the non-balanced dual-echo Dixon acquisitions (Fig. 2b–d). A long TI following the IR pulse (Fig. 2a–c) demonstrated superior suppression of long-T1 tissue species such as synovial fluids in the knee (arrows) compared to the short-TI variant (Fig. 2d). The same long-TI but with an inverted temporal order of the two magnetization-preparation pulses (Fig. 2c) showed reduced background tissue suppression due to signal contamination from short-T2 tissue species such as skeletal muscles (arrow heads). However, a preceding T2-prep pulse in combination with a short TI (Fig. 2d) presented the best quality in terms of uniformity and blood-tissue-contrast over the FOV (dotted arrows). The last variant comprised the proposed REACT method.

By fixing the order of the two pre-pulses as described above, their individual effects were investigated, with different echo times for the T2 preparation pulse and different TIs for the IR pulse. The effect of the T2-prep pulse on background tissue suppression is shown in Fig. 3, where images were acquired with IR-preparation and Dixon TFE in the upper thoracic and abdominal regions. A longer T2-prep echo time led to higher arteriovenous contrast for a fixed TI, as seen between the abdominal aorta and inferior vena cava (arrows). At the same time, lower signal-to-noise level and blood-to-background contrast was also observed (arrow heads). Fig. 4 shows the effect of the IR pulse with associated TI, where images were acquired with T2-preparation and Dixon TFE in abdomen. In general, a longer TI led to poorer blood-to-tissue contrast mainly due to recovery of the background signal, as demonstrated in the signal profile along a horizontal line across the major vessels in the corresponding 2 mm maximum-intensity-projection (MIP) images (Fig. 4b and c). Based on these findings, an echo time of 50 ms for the T2 preparation pulse and a TI of up to 100 ms for the IR pulse were selected for all applications in this work. A joint effect on the final image appearance is demonstrated in Fig. 5.

3.2. REACT vs. conventional NCE-MRA

All data were successfully acquired. Unless otherwise noted, all results are shown as targeted coronal maximum-intensity-projection (MIP) images based on the water-only Dixon data.

Fig. 6 shows the results of comparing REACT with conventional non-contrast-enhanced MRA (NCE-MRA) in healthy volunteers in different body parts. In general, TOF-MRA had difficulty to depict the entire vessels of the subclavian as well as femoral arteries, partially due to its flow-directional sensitivity and surrounding fat signals (dashed arrows). 3D bSSFP-based MRA, though flow independent, failed to depict all vessels in the subclavian, thoracic, and upper abdominal areas, due to either residual motion or banding artifacts typically seen at high field due to susceptibility effects (solid arrows). In addition, inadequate fat suppression and B1 inhomogeneities observed in TRANCE (arrow heads) may lead to difficulty in clinical interpretation [15]. In contrast, REACT showed high blood-to-tissue contrast for all anatomical regions. It is noteworthy that, despite relatively low arterial selectivity, REACT provided the best vessel conspicuity. In particular, it allowed for better visualization of the distal part of the subclavian arteries due to the uniform background tissue suppression (Fig. 6a top right and Fig. 7a), which even permitted a delineation of the corresponding vessels in the arm-abducted position (Fig. 7b). Two other examples in extremities such as hand and foot are presented in Fig. 7c and d, respectively.

3.3. REACT vs. CE-MRA and initial clinical data

A quantitative measurement of CNR between blood and background tissue was shown in Table 2. REACT had a slightly higher overall group mean value than contrast-enhanced MRA (CE-MRA), but there were no significant differences ($p > 0.05$).

Fig. 8 illustrates the comparison between REACT and CE-MRA in patients with vascular malformations of the extremities. In general, REACT showed good image quality, in which all lesions were visible and considered with high conspicuity for all patients. The vascular malformations consisting of dilated tortuous vessels and intramuscular infiltration shown in the CE-MRA were also well depicted by REACT without contrast administration (arrows).

Fig. 9 shows an initial patient study using REACT for renal artery assessment with a comparison to bSSPF-based MRA and digital subtraction angiography (DSA). Due to a history of chronic renal impairment presented with refractory hypertension, the patient was contraindicated from contrast administration. Initial bSSFP-based MRA demonstrated severe stenosis at the proximal third of the left renal artery (arrow) on both axial source and coronal MIP images (Fig. 9a and b). The subsequent free-breathing REACT 8 months later again revealed severe stenosis at the ostium and proximal segment of the left renal artery to a distance of 15 mm from the ostium (Fig. 9c and d). DSA performed on the same day (Fig. 9e) confirmed the finding of severe proximal left renal artery stenosis up to 15 mm from the ostium with good visual correlation, which was followed by successful deployment

Table 2
Quantitative measurement of the contrast-to-noise ratio (CNR) between blood and background tissue for REACT and CE-MRA. See text for details.

Patient index	Anatomies	CNR	
		REACT	CE-MRA
1a	Thigh right	4.16	5.02
1b	Thigh left	2.95	4.36
2	Shoulder	6.55	6.56
3	Arm	10.09	5.20
4a	Subclavian right	4.64	3.82
4b	Subclavian left	3.37	4.18
5	Thigh	3.82	3.99
6	Arm	4.60	6.50
7	Hand	1.52	3.39
8	Thigh	2.76	3.53
9	Thigh	2.33	2.50
10	Arm	4.52	1.39
11	Hand	4.97	3.26
12	Subclavian	13.83	10.61
Mean ± SD		5.01 ± 3.30	4.59 ± 2.37
Paired *t*-test		$P = 0.24$	

of a balloon mounted stent (Fig. 9f).

4. Discussion

We have developed a new technique for relaxation-enhanced MR angiography without contrast and triggering (REACT). The principle of the proposed method is based on non-contrast-enhanced flow-independent angiography (NCE-FIA) with magnetization-preparation [16,17]. However, REACT has its own features differentiating it from the other flow-independent sequences. One of the most distinctive differences is that it exploits the dual-echo generalized Dixon method based on non-balanced gradient echo acquisition to take advantage of robust and uniform fat suppression across a large FOV and 3D volume without banding artifacts, even in challenging anatomical areas and at higher field strengths like 3T. By combining T2 and IR magnetization preparation with a short TI, an efficient background tissue suppression is achieved, which in turn provides a high vessel conspicuity.

The key challenges identified in NCE-FIA so far have been sufficient blood-tissue-contrast, large 3D volume covering complex anatomies (e.g. extremities) with high resolution, and robustness against motion for reduced misalignment. Previously reported approaches utilizing magnetization preparation mainly rely on bSSFP signal acquisition [10,11,18]. Although 3D bSSFP-based signal is flow independent and provides good blood-to-background contrast due to its bright blood signal, it is sensitive to off-resonance effects caused by B0 field inhomogeneities and disruptions of the steady state, such as motion or pulsatile flow. These cause several known drawbacks including banding artifacts, signal loss, residual fat signal, and have restricted its application in the clinical practice, particularly at high field strength [10,11,18]. Notably, such drawbacks persist in the previous attempts using bSSFP Dixon based on either a 3-point approach [19] or center frequency offsets [20,21]. The former is restrained by potential limit of echo spacing at 3T as well as patient motion due to long TR (10 ms) and scan time (typically 6 to 8 min) [19], whereas the latter has limited FOV coverage and also flip angle restrictions due to an increased specific absorption rate (SAR) [20,21]. These limitations are largely overcome in this work by employing the Dixon method in a combination of non-balanced gradient-echo acquisition and 2-point generalized solution with semi-flexible echo times, which potentially also results in a shorter TR. This Dixon method is tolerant to field inhomogeneity and tissue susceptibility differences, as previously also shown in subtraction-less CE-MRA [32]. It provides a robust fat suppression over a large FOV in complex anatomies such as the subclavian area or extremities (Figs. 6 to 8) and allows for high-resolution, large-coverage acquisition with reasonable scan times (approximately 3 to 4 min), even at 3T.

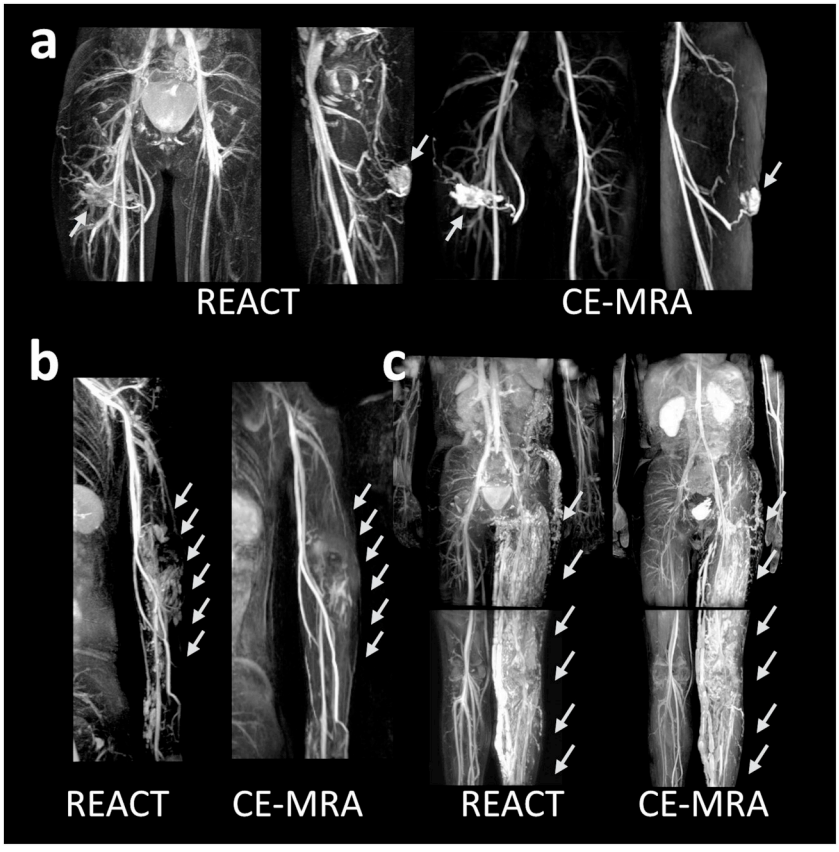

Fig. 8. REACT in patients with comparison to contrast-enhanced MRA. Representative examples were selected from different patients with vascular malformation at right femur (**a**), left arm extending from shoulder down to the wrist (**b**), and left leg extending along the entire limb (**c**). REACT presented good image quality and also visualized equivalent clinical indication for dilated tortuous vessels and intramuscular infiltration (arrows). Details of the CE-MRA imaging parameters see Table 1.

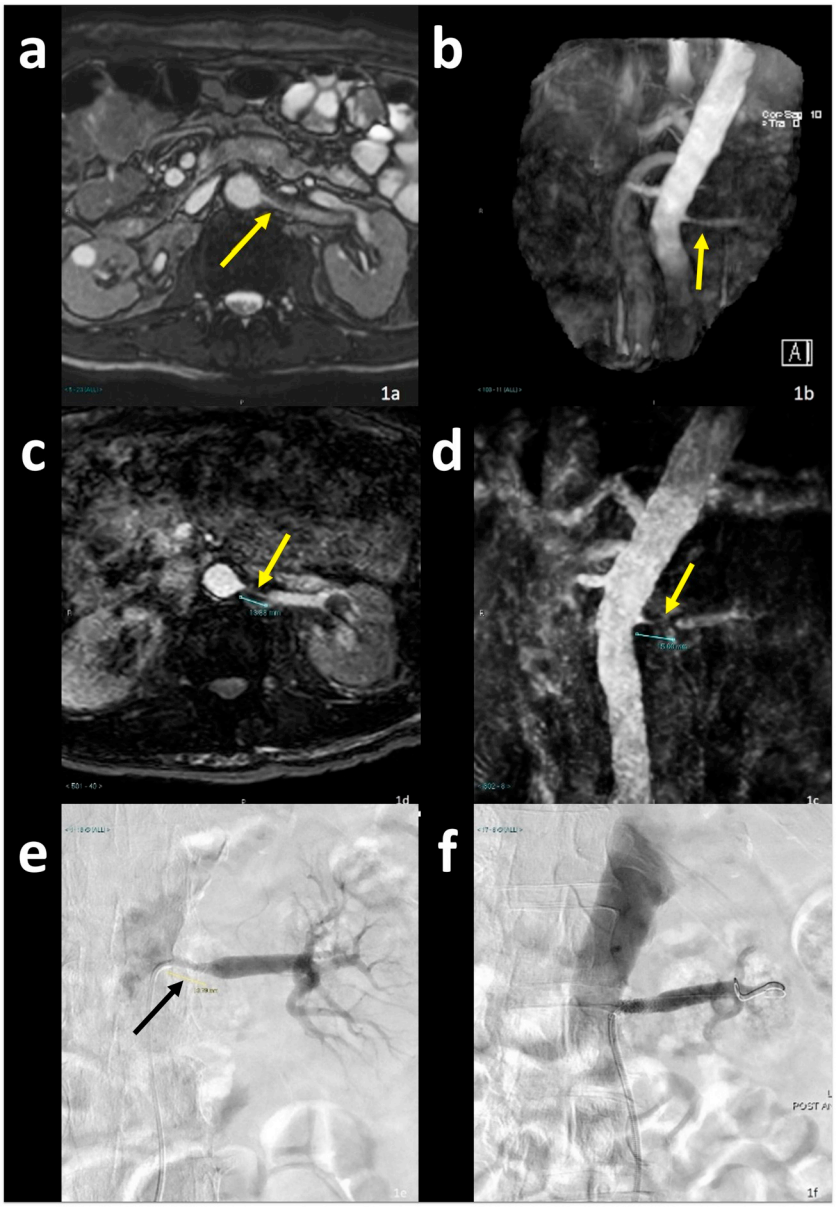

Fig. 9. REACT for renal artery assessment in a patient with chronic renal impairment (male, 72 years old). In both source images (**a**, **c**) and coronal MIP (**b**, **d**) of the initial bSSFP-based MRA (**a**, **b**) and REACT (**c**, **d**), with 8 months apart, severe stenosis in the left renal artery can be well demonstrated (arrow). Digital subtraction angiography (DSA) performed on the same day of REACT confirmed this finding with good visual correlation (**e**), followed by successful deployment of a balloon mounted stent (**f**).

Compared to the other magnetization-prepared NCE-FIA techniques [10,11,18,19], another difference of the current method is the inverted temporal order of the IR and T2 pulses. An IR pulse with a long inversion time (TI) that precedes the T2-prep pulse helps to attenuate long-T1 fluids, as shown in Fig. 2 and also previously described [10,11,33]. However, the fact that the thoracoabdominal area contains organs and tissues with mixed T1 times has limited its application mainly to peripheral angiography [10,11,18,19]. In addition, a long TI results in a lower SNR and blood-tissue-contrast in general, as observed in Fig. 4. In contrast, in this work the IR pulse was implemented immediately after the T2-prep pulse with a short TI, mainly serving to nulling the static tissues with short-to-intermediate T1 and T2. This is important because for tissue with a relatively short T2 and thus suppressed by the T2-prep pulse, such as muscle or internal organs, only a short TI is needed to null out its residual signal (Figs. 1 and 4). Although this results in low artery-to-vein contrast and bright signal from the long-T1 fluids such as edema, cerebrospinal fluid (CSF) or synovial fluid, as previously described in an early study [9], it provides the best quality with a robust blood-tissue-contrast in general (Fig. 2). The residual signal from fat is further suppressed by the dual-echo generalized Dixon method to enhance the blood-to-tissue contrast (Figs. 3 to 5).

Moreover, the comparison study in healthy volunteers (Fig. 6) shows that REACT can better depict all vessels within the FOV with a shorter scan time, in comparison to the flow-dependent MRA techniques such as TOF or TRANCE. These two techniques also require ECG gating either to avoid ghost artifacts from periodic view-to-view variations in arterial signal (e.g. for 2D TOF) [14] or to ensure that data are specifically acquired during peak systolic and diastolic phases of the cardiac cycle (e.g. for TRANCE) [15]. In the latter case, as an angiogram is obtained via subtraction of two measurements, motion-induced misalignment could potentially limit the robustness of the method and cause a significant problem in patient exams. This challenge also applies to the recently proposed velocity-selective or acceleration-dependent approaches [34–36] and dual-acquisition methods

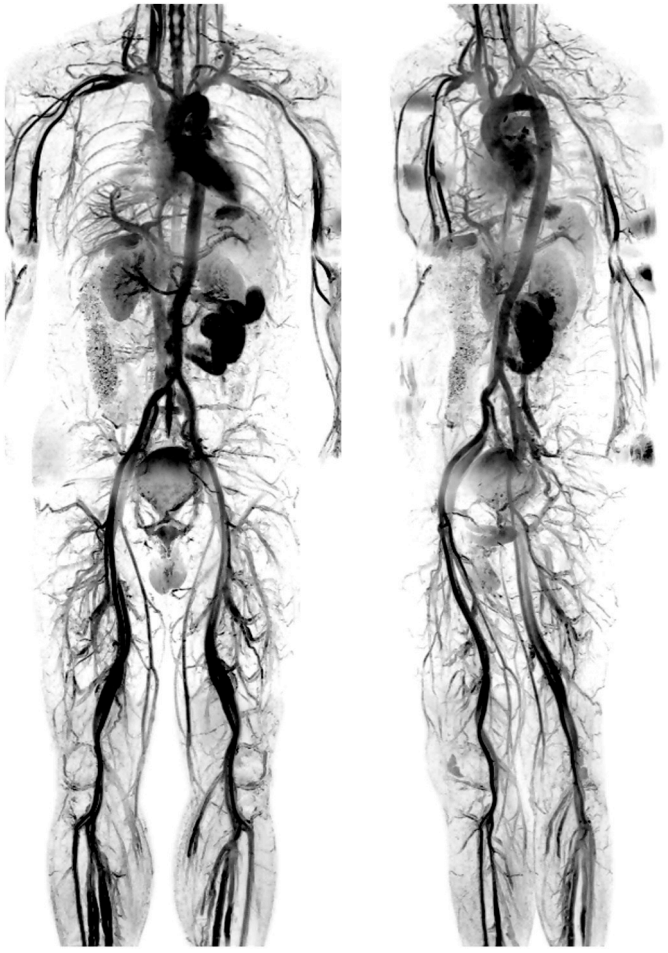

Fig. 10. REACT for non-contrast-enhanced whole-body free-breathing MRA in a healthy volunteer. The angiogram was produced in four stations: thorax, abdomen, thigh and calf, respectively. Detailed depiction of the vasculature was achieved through 3D high-resolution isotropic acquisitions. The coronal and oblique-coronal views with inverted image contrast were shown here.

[10,20,21,37]. REACT, however, as a flow-independent and subtraction-less technique, achieve proper vessel delineation in lower extremities without the need for cardiac synchronization. Recently, another NCE-MRA technique based on inflow-preparation and multi-slice bSSFP readout, termed quiescent-interval slice-selective (QISS), has also demonstrated its capability for whole-body angiogram on 1.5T [38–41]. However, its bSSFP readout poses associated challenges such as banding artifacts for applications on 3T [42]. Alternative implementations like non-bSSFP readout may help to improve its robustness at a potential cost of lower SNR [43]. A systematic investigation would be required in future studies for a direct comparison with the current method.

In the clinical setting, removing the need for contrast injection is especially important for patients with, for example, severe renal parenchymal impairment, pregnancy or young age. A robust high-quality free-breathing NCE-MRA technique, which can be performed "on-the-fly" without the need for applying respiratory sensors or ECG electrodes, and within a reasonable scan time is invaluable. Initial patient studies in Figs. 8 and 9 demonstrate a strong visual correlation between REACT and other conventional angiographic imaging, with better diagnostic quality from REACT in some cases. CE-MRA typically requires certain waiting time to visualize vascular malformation, given a "delayed effect" due to contrast filling. REACT, being a NCE-MRA method, eliminates such an acquisition time window dependence, and further allows for a clear delineation of the overall internal extent of the lesion. It shows a promising potential in the clinical assessment of vascular malformations or vasculopathies [44,45] and pediatric applications [46]. In particular, REACT may help to serve as an initial "survey", for example, in multiple-station whole body screening as demonstrated in Fig. 10, for any further targeted imaging. However, as with any other NCE-MRA methods, where the image characteristics in patients may not necessarily be the same as that of CE vascular imaging technique [17], its clinical performance in diagnosis or treatment monitoring needs to be further investigated in an extended patient cohort.

There are several limitations to the proposed REACT method. First, both arteries and veins were visible in the results presented. Our results have shown that the relaxation time difference between arterial and venous blood, due to difference in their oxygenation levels, can be further exploited for improved arteriovenous contrast by prolonging the T2-preparation echo time (Fig. 3). This has also been shown in the other flow-independent angiography methods in NCE-MRA [19,47]. Unfortunately, however, it also caused lower blood-to-tissue contrast and lower signal-to-noise level that might lead to potential failure in water-fat separation [9,45]. Nevertheless, in most clinical situations it is usually straightforward to visually distinguish arteries from veins. In certain cases the ability to assess venous anatomy can even prove to be an advantage, such as for evaluation of complex arteriovenous malformations and other non-ischemic vascular diseases, e.g. in pediatric patients. While further investigations are needed to evaluate the optimal T2-prep echo times, an acceleration-dependent preparation approach may help to improve artery sensitization and remove venous "contamination" for potential simplification in clinical interpretation [19]. Second, bright signal of long-T1 fluids such as edema, CSF or synovial fluid are visible in the REACT images (Fig. 2). This can obscure vascular structure in the region of interest, has also been observed with the bSSFP-based methods [10,11,18]. On the other hand, it is also clinically relevant to have such information present in the angiogram, as shown in Fig. 8. An improved suppression of this long-T1 fluid signal could potentially be achieved by selecting parameter sets including different TI times as well as exciting flip angles as described in [9]. A more comprehensive study must be undertaken to evaluate these effects and to fully compare the relative benefits of magnetization preparation and signal readout methods, as it is well known that relaxation-based NCE-MRA must trade-off between improving the quality of surrounding stationary tissue suppression at the cost of arterial signal loss [17].

Another improvement of our proposed technique would be to combine existing motion compensation approaches such as respiratory triggering for a further detailed vessel delineation [46]. Although this may increase the scan time, we expect that imaging acceleration techniques like compressed sensing, taking advantage of the inherent sparsity of MR angiograms, may preserve or shorten the total scan duration even with respiratory triggering [48,49]. In addition, the proposed REACT method can be easily extended to 1.5T, where less challenges in field homogeneity are present.

In conclusion, we have demonstrated the feasibility of REACT as a new non-contrast-enhanced relaxation-based flow-independent MRA method for vascular imaging in various body parts with large anatomical coverage at 3T. Initial results in both healthy subjects and patients show high-quality angiograms with robust uniform fat suppression in complex anatomies and good blood-to-tissue contrast. Future investigations should focus on an improved artery-vein-contrast, and further studies are warranted to assess the clinical utility of this method in patients with suspected vascular pathologies and its diagnostic performance in comparison to other MRA techniques.

Acknowledgement

The authors thank Jonathan Chia, Philips USA for collaborative work in the early stage of this work.

Grant support

No

References

[1] Prince MR. Gadolinium-enhanced MR aortography. Radiol 1994;191:155–64.
[2] Korosec FR, Frayne R, Grist TM, Mistretta CA. Time-resolved contrast-enhanced 3D MR angiography. Magn Reson Med 1996;36:345–51.
[3] Hartung MP, Grist TM, Franc¸ois CJ. Magnetic resonance angiography: current status and future directions. J Cardiovasc Magn Reson 2011;13:19.
[4] Zhang H, Maki JH, Prince MR. 3D contrast-enhanced MR angiography. J Magn Reson Imaging 2007;25:13–25.
[5] Ivancevic MK, Geerts L, Weadock WJ, Chenevert TL. Technical principles of MR angiography methods. Magn Reson Imaging Clin N Am 2009;17:1–11.
[6] Thomsen HS. Nephrogenic systemic fibrosis: a serious late adverse reaction to gadodiamide. Eur Radiol 2006;16:2619–21.
[7] Kuo PH, Kanal E, Abu-Alfa AK, Cowper SE. Gadolinium-based MR contrast agents and nephrogenic systemic fibrosis. Radiol 2007;242:647–9.
[8] Edelman RR, Koktzoglou I. Noncontrast MR angiography: an update. J Magn Reson Imaging 2018. https://doi.org/10.1002/jmri.26288.
[9] Brittain JH, Olcott EW, Szuba A, et al. Three-dimensional flow-independent peripheral angiography. Magn Reson Med 1997;38:343–54.
[10] Çukur T, Lee JH, Bangerter NK, Hargreaves BA, Nishimura DG. Non-contrast-enhanced flow-independent peripheral MR angiography with balanced SSFP. Magn Reson Med 2009;61:1533–9.
[11] Bangerter NK, Cukur T, Hargreaves BA, et al. Three-dimensional fluid-suppressed T2-prep flow-independent peripheral angiography using balanced SSFP. Magn Reson Imaging 2011;29:1119–24.
[12] Katoh M, Spuentrup E, Stuber M, Hoogeveen R, Gunther RW, Buecker A. Free-breathing renal magnetic resonance angiography with steady-state free-precession and slab-selective spin inversion combined with radial k-space sampling and water-selective excitation. Magn Reson Med 2005;53:1228–33.
[13] Shimada K, Isoda H, Okada T, et al. Non-contrast-enhanced MR angiography for selective visualization of the hepatic vein and inferior vena cava with true steady-state free-precession sequence and time-spatial labeling inversion pulses: preliminary results. J Magn Reson Imaging 2009;29:474–9.
[14] Vosshenrich R, Kopka L, Castillo E, Boettcher U, Graessner J, Grabbe E. Electrocardiograph-triggered two-dimensional time-of-flight versus optimized contrast-enhanced three-dimensional MR angiography of the peripheral arteries. Magn Reson Imaging 1998;16:887–92.
[15] Gutzeit A, Sutter R, Froehlich JM, et al. ECG-triggered non-contrast-enhanced MR angiography (TRANCE) versus digital subtraction angiography (DSA) in patients with peripheral arterial occlusive disease of the lower extremities. Eur Radiol 2011;21:1979–87.
[16] Blankholm AD, Ringgaard S. Non-contrast-enhanced magnetic resonance angiography: techniques and applications. Expert Rev Cardiovasc Ther 2012;10:75–88.
[17] Wheaton AJ, Miyazaka M. Non-contrast enhanced MR angiography: physical principles. J Magn Reson Imaging 2012;36:286–304.
[18] Kwon KT, Kerr AB, Wu HH, et al. Non-contrast-enhanced peripheral angiography using a sliding interleaved cylinder acquisition. Magn Reson Med 2015;74:727–38.
[19] Cukur T, Shimakawa A, Yu H, et al. Magnetization-prepared IDEAL bSSFP: a flow-independent technique for noncontrast-enhanced peripheral angiography. J Magn Reson Imaging 2011;33:931–9.
[20] Stafford RB, Sabati M, Mahallati H, Frayne R. 3D non-contrast-enhanced MR angiography with balanced steady-state free precession Dixon method. Magn Reson Med 2008;59:430–3.
[21] Stafford RB, Sabati M, Haakstad MJ, Mahallati H, Frayne R. Unenhanced MR angiography of the renal arteries with balanced steady-state free precession Dixon method. Am J Roentgenol 2008;191:243–6.
[22] Eggers H, Brendel B, Duijndam A, Herigault G. Dual-echo Dixon imaging with flexible choice of echo times. Magn Reson Med 2011;65:96–107.
[23] Eggers H, Börnert P. Chemical shift encoding-based water-fat separation methods. J Magn Reson Imaging 2014;40:251–68.
[24] Diefenbach MN, Ruschke S, Eggers H, Meineke J, Rummeny EJ, Karampinos DC. Improving chemical shift encoding-based water-fat separation based on a detailed consideration of magnetic field contributions. Magn Reson Med 2018;80:990–1004.
[25] Kijowski R, Woods MA, Lee KS, et al. Improved fat suppression using multipeak reconstruction for IDEAL chemical shift fat-water separation: application with fast spin echo imaging. J Magn Reson Imaging 2009;29:436–42.
[26] Eggers H, Perkins TG, Hussain SM. Influence of spectral model and signal decay on hepatic fat fraction measurements at 3 T with dual-Echo Dixon imaging. Proceedings of the 19th annual meeting Intl Soc mag Reson med (ISMRM), Montreal, Canada. 2011. p. 573.
[27] Perkins TG, Tilburg JLV, Herigault G, et al. Preliminary clinical experience with a multiecho 2-point DIXON (mDIXON) sequence at 3T as an efficient alternative for both SAR-intensive acquired in- and out-of-phase chemical shift imaging as well as for 3D fat-suppressed T1-weighted sequences used for dynamic gadolinium-enhanced imaging. Proceedings of the 18th annual meeting of Intl Soc Mag Reson Med (ISMRM), Stockholm, Sweden. 2010. p. 1238.
[28] Andia ME, Henningsson M, Hussain T, et al. Flow-independent 3D whole-heart vessel wall imaging using an interleaved T2-preparation acquisition. Magn Reson Med 2013;69:150–7.
[29] Shonai T, Takahashi T, Ikeguchi H, Miyazaki M, Amano K, Yui M. Improved arterial visibility using short-tau inversion-recovery (STIR) fat suppression in non-contrast-enhanced time-spatial labeling inversion pulse (time-SLIP) renal MR angiography (MRA). J Magn Reson Imaging 2009;29:1471–7.
[30] Vlaardingerbroek MT, Boer JA. Magnetic resonance imaging: Theory and practice. Springer Science & Business Media; 2004. [252-255 p].
[31] Storey P, Atanasova IP, Lim RP, et al. Tailoring the flow sensitivity of fast spin-echo sequences for noncontrast peripheral MR angiography. Magn Reson Med 2010;64:1098–108.
[32] Leiner T, Habets J, Versluis B, et al. Subtractionless first-pass single contrast medium dose peripheral MR angiography using two-point Dixon fat suppression. Eur Radiol 2013;23:2228–35.
[33] Epstein FH, Mugler JP, Cail WS, Brookeman JR. CSF-suppressed T2-weighted three dimensional MP-RAGE MR imaging. J Magn Reson Imaging 1995(4):463–9.
[34] Priest AN, Graves MJ, Lomas DJ. Non-contrast-enhanced vascular magnetic resonance imaging using flow-dependent preparation with subtraction. Magn Reson Med 2012;67:628–37.
[35] Shin T, Worters PW, Hu BS, Nishimura DG. Non-contrast-enhanced renal and abdominal MR angiography using velocity-selective inversion preparation. Magn Reson Med 2013;69:1268–75.
[36] Priest AN, Taviani V, Graves MJ, Lomas DJ. Improved artery–vein separation with acceleration-dependent preparation for non-contrast-enhanced magnetic resonance angiography. Magn Reson Med 2014;72:699–706.
[37] Hargreaves BA, Bangerter NK, Shimakawa A, Vasanawala SS, Brittain JH, Nishimur DG. Dual-acquisition phase-sensitive fat–water separation using balanced steady-state free precession. Magn Reson Imaging 2006;24:113–22.
[38] Edelman RR, Sheehan JJ, Dunkle E, et al. Quiescent-interval single-shot unenhanced magnetic resonance angiography of peripheral vascular disease: technical considerations and clinical feasibility. Magn Reson Med 2010;63:951–8.
[39] Hodnett PA, Koktzoglou I, Davarpanah AH, et al. Evaluation of peripheral arterial disease with nonenhanced quiescent-interval single-shot MR angiography. Radiol 2011;260:282–93.
[40] Nose K, Sakai T, Ochi S, Yanagawa N. Examination of lower-extremity MRA using single-shot balanced SSFP with saturation recovery. J Japan Soc Radiol Technol. 2017;73:1252–1257. doi: 10.6009/jjrt.2017_JSRT_73.12.1252.
[41] Varga-Szemes A, Wichmann JL, Schoepf JS, et al. Accuracy of noncontrast quiescent-interval single-shot lower extremity MR angiography versus CT angiography for diagnosis of peripheral artery disease. Comparison with digital subtraction angiography. JACC Cardiovasc Imaging 2017(10):1116–24.
[42] Hanrahan CJ, Lindley Mueller M, et al. Diagnostic accuracy of noncontrast MR angiography protocols at 3T for the detection and characterization of lower extremity peripheral arterial disease. J Vasc Interv Radiol 2018;29:1585–94.
[43] Edelman RR, Carr M, Koktzoglou I. Advances in non-contrast quiescent-interval slice-selective (QISS) magnetic resonance angiography. Clin Radiol 2019;74:29–36.
[44] Toyonari N, Yoneyama M, Noda S, Horino Y, Katahira K. Non-contrast gate-free aortic MR angiography with robust fat suppression. Proceedings of the 24th annual meeting Intl Soc Mag Reson Med (ISMRM), Singapore. 2016. p. 2684.
[45] Yoneyama M, Toyonari N, Noda S, Horino Y, Katahira K, Van Cauteren M. Non-contrast, flow-independent, relaxation-enhanced subclavian MR angiography using inversion recovery and T2 prepared 3D gradient-echo DIXON sequence. Proceedings of the 24th annual meeting Intl Soc Mag Reson Med (ISMRM), Singapore. 2016. p. 2252.
[46] Dillman JR, Trout AT, Merrow AC, Moore RA, Rattan MS, Crotty EJ, et al. Non-contrast three-dimensional gradient recalled echo Dixon-based magnetic resonance angiography/venography in children. Pediatr Radiol 2019;49:407–14.
[47] Brittain JH, Hu BS, Wright GA, et al. Coronary angiography with magnetization-prepared T2 contrast. Magn Reson Med 1995;33:689–96.
[48] Lustig M, Donoho DL, Pauly JM. Sparse MRI: the application of compressed sensing for rapid MR imaging. Magn Reson Med 2007;58:1182–95.
[49] Çukur T, Lustig M, Nishimura DG. Improving non-contrast-enhanced steady-state free precession angiography with compressed sensing. Magn Reson Med 2009;61:1122–31.
[50] Aubert B, Bakker CJG, Bernard AM, et al. EEC concerted research project. Protocols and test objects for the assessment of MRI equipment. Magn Reson Imaging 1988;6:195–9.